Am J Transl Res 2017;9(3):1344-1356
www.ajtr.org /ISSN:1943-8141/AJTR0042745

Original Article

Neuroprotective effect of miR-665 against sevoflurane anesthesia-induced cognitive dysfunction in rats through PI3K/Akt signaling pathway by targeting insulin-like growth factor 2

Xihua Lu, Shuaiguo Lv, Yan Mi, Lei Wang, Gensheng Wang

Department of Anesthesiology, Affiliated Cancer Hospital of Zhengzhou University, Henan Cancer Hospital Anesthesiology, Zhengzhou 450003, Henan, China

Received October 24, 2016; Accepted February 7, 2017; Epub March 15, 2017; Published March 30, 2017

Abstract: The aim of this study was to investigate the *in vivo* and *in vitro* effects of miR-665 on sevoflurane anesthesia-induced cognitive dysfunction. SH-SY5Y cells and male SD rats were treated with sevoflurane to simulate anesthesia-induced cognitive dysfunction. The cells and rats both were transfected with a miR-665 mimic, inhibitor, scramble, IGF-2 siRNA, or treated with P13K/Akt inhibitor LY294002. The cell apoptosis, autophagy, growth related proteins, and mRNA levels were measured using different methods. The motor performance was assessed using the Morris water maze (MWM) test. Finally, the differences were statistically analyzed. It was noted that sevoflurane-induced miR-665 downregulation accompanied with the upregulation of IGF-2 *in vivo* and motor deficits *in vitro*. Moreover, sevoflurane also induced hippocampal neuroapoptosis; reduced regular autophagy; increased Bax/Bcl-2 ratio; decreased the expression of Beclin 1, PSD95, and p-CREB; and activated P13K/Akt signaling pathway. However, the treatment by miR-665 mimics significantly reversed all the molecular changes and improved motor performance. Our data demonstrate the neuroprotective effect of miR-665 against sevoflurane anesthesia-induced cognitive impairment. This study suggests that miR-665 might be explored as a potential target of therapy for sevoflurane-induced cognitive impairment.

Keywords: miR-665, insulin-like growth factor 2, neuron apoptosis, P13k/Akt

Introduction

Old-aged individuals with Alzheimer's disease and those have received anesthesia or undergone surgery usually suffer from cognitive dysfunction or impairment [1, 2]. Elderly people with nerve diseases are always a high-risk population for cognitive dysfunction [3, 4]. Abnormal alterations and accumulation of genetic or non-genetic elements are the main inducements of cognitive dysfunction and impairments; therefore, the complete therapy of cognitive impairments in elderly people is an arduous process with a limited success [5].

Several lines of evidence have shown that cognitive impairments caused by surgical anesthesia or brain trauma are associated with dysregulation of signaling pathways, such as an inactivation of P13K/Akt and extracellular signal-regulated kinase 1/2 (ERK1/2) signaling pathways [6, 7] and enhanced neuroapoptosis or neurotoxicity resulting by these dysregulations [7, 8]. As reported earlier, neuroapoptosisis also linked to abnormal alterations of postsynaptic density protein (PSD)-95 [9], cyclic adenosine monophosphate (cAMP)-response element binding protein (CREB) [10], brain-derived neurotrophic factor (BDNF) [11], and dysregulation of microRNAs (miRNAs) including miR-34a [12], miR-383 [13], and miR-665 [14].

miRNA are small noncoding RNAs. They play an important role in metabolism, thus their abnormal transcription results in certain diseases [15, 16]. Many of these miRNAs have been used as a specific biomarker for diseases, such as miR-21 and miR-383 in lung cancer [17, 18], miR-210 in congestive heart failure and glioma [19, 20], and miR-665 in con-

gestive heart failure [21]. Recently, numerous miRNAs have been identified to be associated with anesthesia-related cognitive dysfunction such as miR-665 [14, 22], miR-572 [23], and miR-181 [24]. Therefore, miRNA can be targeted for potential therapeutic approaches for the related diseases [24, 25]. For example, the downregulation of miR-383 promoted cancer cell proliferation and invasion [26], and miR-665 expression showed the neuroprotective effect on propofol-induced cognitive dysfunction in a rat model [14]. However, there is no evidence showing the effect of sevoflurane anesthesia-induced cognitive impairment on miR-665 expression and the associated mechanism.

In order to investigate the effect of miR-665 expression on sevoflurane-induced learning and memory impairment, we established a cognitive impairment rat model using sevoflurane. The effects of miR-665 expression on the sevoflurane-anesthetized cognitive impairment were studied using constructed lentivirus vectors expressing miR-665 mimics. Neuroapoptosis, the expression of related proteins, rat learning and memory ability, and the cognitive performance were monitored to glean more information on the mechanism of sevoflurane-anesthetized cognitive impairment and the potential of targeting miR-665 for a therapeutic strategy.

Materials and methods

Cell line and cell culture

Human neuronal SH-SY5Y neuroblastoma cells were procured from ATCC (Manassas, VA, USA) and cultured in Dulbecco's Minimum Essential Medium (DMEM) (Sigma, St. Louis, MO, USA), containing 10% fetal bovine serum (FBS; Sigma, St. Louis, MO, USA) and 100 U/mL penicillin (Sigma, St. Louis, MO, USA) at 37°C with 5% CO_2, using the 96-well plates (BD Biosciences, Rockville, MD).

Cell transfection

The SH-SY5Y cells were pretreated with 5, 10, 20, and 30 μM sevoflurane (AbbVie Inc., North Chicago, IL, USA) for 30 min for *in vitro* experiments [27]. In addition, the cells were pretreated with PI3K/Akt pathway inhibitor LY294-002 (Sigma, St. Louis, MO, USA) for 30 min as described previously [28]. The cells were plated in 6-well plates (BD Biosciences, Rockville, MD). MiR-665 inhibitor/mimic/scramble (Ambion, Foster City, CA, USA), and chemical siRNA sequences against insulin-like growth factor 2 (IGF-2, Ambion, a miR-665 target predicted using Target Scan Human: http://www.targetscan.org/vert_71/) were used for cell transfection. The transfections of these molecules were performed using Lipofectamine 2000 (Invitrogen, Carlsbad, CA) or lentivirus. The SH-SY5Y cells transfected with scramble or Lipofectamine 2000 were considered as controls.

Animal model

All protocols of animal experiments were reviewed and approved by the Institutional Animal Care and Use Committee at the Affiliated Cancer Hospital of Zhengzhou University, Henan Cancer Hospital Anesthesiology, Henan, China. Before the experiments, Sprague-Dawley rats (male, 250 ± 10 g, seven-week-old; Vital River Laboratory Animal Technology Co. Ltd., Beijing, China) were housed under a controlled 12 D:12 L cycle condition for seven days with ad libitum access to food and water. The rats were then randomly divided into two groups: a control group receiving regular air inhalation for 6 h and a sevoflurane group receiving 2.5% sevoflurane at 600 $\mu g \cdot kg^{-1} \cdot min^{-1}$ in 100% O_2 at the identical conditions for 6 h. The animals were allowed for recovery for seven days after the anesthesia. For animal transfections, lentivirus-miR-665 inhibitor/mimic/scramble and lentivirus-siRNA-IGF-2 were given intracerebroventricularly into the left lateral cerebral ventricles through a pre-drilled skull hole within 10 min after sevoflurane administration [29].

Morris water maze task

The Morris water maze (MWM) test was used to examine spatial learning and memory of rats [30]. In brief, each rat was forced to finish a swim test every day subsequently from each of the four quadrants per day for five days from each of the four quadrants in a circular water pool (colored with black ink, 100 cm in diameter, 50 cm in height) with a 30-cm depth of water and a hidden circular platform (12 cm in diameter) 2 cm below the water surface. The animals were forced to finish swim to find the hidden platform within a maximum of 60 s. The

Table 1. Primer list used in this study for qRT-PCR detection

Gene names	Primers	Sequences (5'-3')
miR-665	Forward	5'-ACCAGGAGGCTGAGG-3'
	Reverse	5'-GAGCAGGCTGGAGAA-3'
	RT primer	5'-GCGCGTGAGCAGGCTGGAGAAATTAACCACGCGCTAAGGG-3'
Bcl-2	Forward	5'-GGTGAACTGGGGGAGGATTG-3'
	Reverse	5'-GCATGCTGGGGCCATATAGT-3'
Bcl-xL	Forward	5'-GGACAGCATATCAGAGCTTTGAACA-3'
	Reverse	5'-TTGTCTACGCT TTCCACGCA-3'
Bax	Forward	5'-GGCTGGACACTGGACTTCCT-3'
	Reverse	5'-GGTGAGGACTGGAGCCACAA-3'
Beclin 1	Forward	5'-GAGAGGAGCCATTTATTGAAAC-3'
	Reverse	5'-CTCCCCAATCAGAGTGAAGC-3'
PSD-95	Forward	5'-TAGGGCCCTGTTTGATTACG-3'
	Reverse	5'-TGGCCTTTAACCTTGACCAC-3'
Caspase-3	Forward	5'-AATTCAAGGGACGGGTCATG-3'
	Reverse	5'-GCTTGTGCGCGTACAGTTTC-3'
IGF-2	Forward	5'-GAGAACCTTCCAGCCTTT-3'
	Reverse	5'-GAGATGAGAAGCACCAACA-3'
GAPDH	Forward	5'-GGGCAAGGTCATCCCTGAGCTGAA-3'
	Reverse	5'-GAGGTCCACCACCCTGTTGCTGTA-3'
U6	Forward	5'-CTCGCTTCGGCAGCACA-3'
	RT and reverse	5'-GTGCA GGGTCCGAGGT-3'

time each rat spent to find the hidden platform for the first time on day 5 of the trials (latency) was recorded to evaluate the learning ability of the rats [30]. A video camera on the ceiling was used to record the performances of the rats related to swim ability. The time taken to find the hidden platform (latency, s), path length (cm), and swimming speeds ($cm \cdot s^{-1}$) were analyzed using image tracking software (2020 Plus Tracking System; HVS Image).

qRT-PCR

In order to carry out the qRT-PCR analysis, total RNA was extracted from the cells and rat hippocampus tissues using Trizol (Invitrogen, Carlsbad, CA, USA) after seven days of the last injection of MWM task. The single-strand cDNA was then synthesized and the expression levels of genes and miRNAs were determined by using a Bio-Rad SsofastEvaGreenSupermixkit (Bio-Rad Laboratories, Hercules, CA, USA) with Bio-Rad IQ5 real-time PCR system (Bio-Rad). Primers for qRT-PCR (Sangon, Shanghai, China) are listed in **Table 1**. β-Actin and U6 were used as the internal reference genes for mRNA and miRNA detection, respectively.

Western blotting

The Western blotting was performed using antibodies specific for postsynaptic density-95 (PSD-95, 1:1000 dilution, Cell Signaling Technology, CST, Danvers, MA, USA), cyclic adenosine monophosphate (cAMP)-response element binding protein (CREB, CST, 1:1000 dilution), and phospho-CREB (p-CREB, CST, 1:1000 dilution), p-PI3K (CST, 1:1000 dilution), p-Akt (CST, 1:1000 dilution), PI3K (CST, 1:5000 dilution), Akt (CST, 1:1000 dilution) and GAPDH (1:2000 dilution, Sizhengbo, Beijing, People's Republic of China). For the Western blot, the mice were killed and hippocampus tissue proteins were extracted, and the cellular proteins were prepared as described previously. Protein concentrations were determined by Bio-Rad DC protein assay, and subsequently, the proteins were separated on 12% SDS-PAGE. The protein blots were transblotted onto polyvinylidene difluoride membranes (PVDF; Millipore, Billerica, MA, USA), which were then blocked and incubated with the specific primary antibodies at 4°C overnight, and HRP-conjugated secondary antibodies for 1 h. Immunoreactive protein bands were visualized by a chemiluminescence reac-

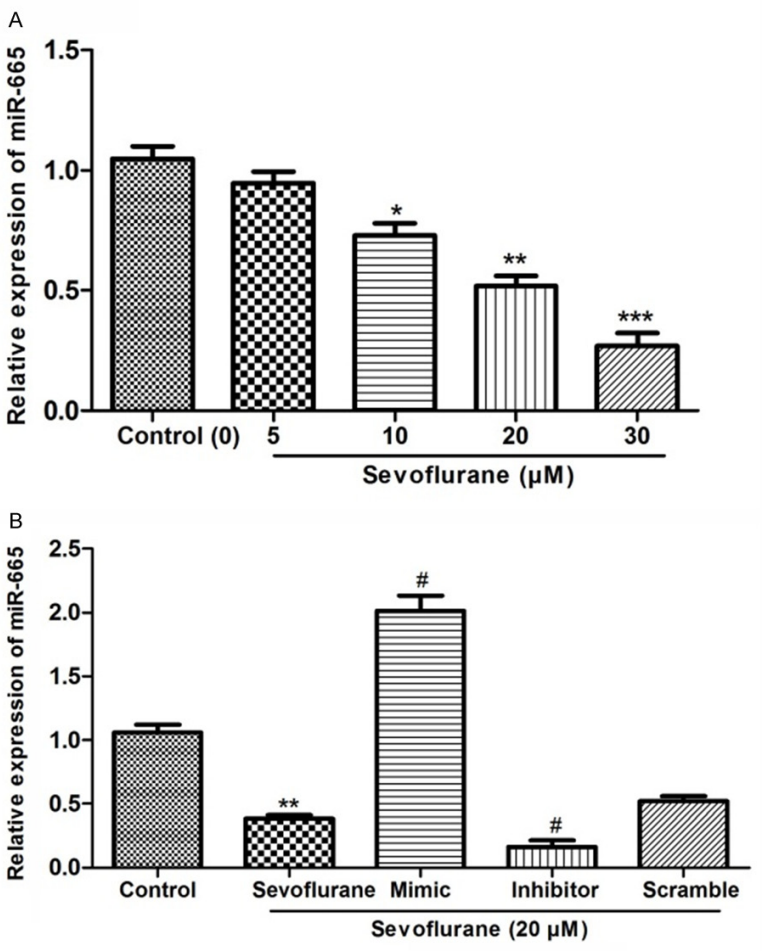

Figure 1. Sevoflurane inhibits miR-665 expression in SH-SY5Y cells. A. SH-SY5Y cells treated with 5, 10, 20, and 30 μM sevoflurane. B. SH-SY5Y cells treated with 20 μM sevoflurane and then transfected with miR-665 mimic, inhibitor, and scramble for 24 h. The expression level of miR-665 was detected using qRT-PCR. * and **indicate difference at $P < 0.05$ and $P < 0.01$, vs. control, respectively. #Indicates difference at $P < 0.05$ vs. sevoflurane control.

tion, and the data were analyzed using the Bio-Rad Quantity One software (Bio-Rad, Richmond, CA, USA).

Apoptosis assay

Apoptosis in the transfected cells was detected using an annexin V-Cy5-labeled apoptosis detection kit (Invitrogen) and analyzed by flow cytometry [31]. Briefly, after being transfected with miR-665 mimic/inhibitor/scramble and siRNA-EGF-2 or control for 24 h, the cells were harvested, pelleted, and resuspended in the binding buffer containing annexin V-Cy5 (1:1000) and propidium iodide (PI) for 10 min. Then the cells were analyzed using a FACS Calibur flow cytometer (Becton-Dickinson, CA, USA). Annexin V-Cy5 positive and PI-negative cells (Annexin V+/PI-, early apoptotic cells) were considered to be apoptotic cells.

Dual-luciferase reporter analysis

The reporter vectors of pGL3-IGF-2-3'-UTR were synthesized (Sangon Biotech, Shanghai, China) and dual-luciferase (Firefly and Renilla) reporter plasmids IGF-2-WT and IGF-2-Mut, containing the wild-type and mutant IGF-2 putative 3'-UTR-binding site, respectively, were constructed. After cell transfection for 48 h, luciferase activities were measured using the Promega Dual-luciferase Reporter Assay kit (Promega, Madison, WI). Fold induction of firefly luciferase activity was normalized to Renilla-luciferase activity for each sample [32].

Statistical analysis

All statistical analyses were performed using SPSS 19.0 software (SPSS Inc., Chicago, USA). All data were expressed as the mean ± standard deviation (SD). The differences between two groups and among more than two groups were analyzed using Tukey's test and ANOVA, respectively. $P < 0.05$ was considered statistically significant. The plots were made using GraphPad Prism 6.0 (GraphPad Software Inc, La Jolla, CA, USA).

Results

Sevoflurane inhibited miR-665 expression in vitro

SH-SY5Y cells were treated with 5, 10, 20, and 30 μM sevoflurane and the expression of miR-665 was detected using qRT-PCR. The expression level of miR-665 was decreased in the sevoflurane-treated cells in a concentration-dependent manner (**Figure 1A**). Sevoflurane at 10, 20, and 30 μM concentrations significantly inhibited miR-665 expressions ($P <$

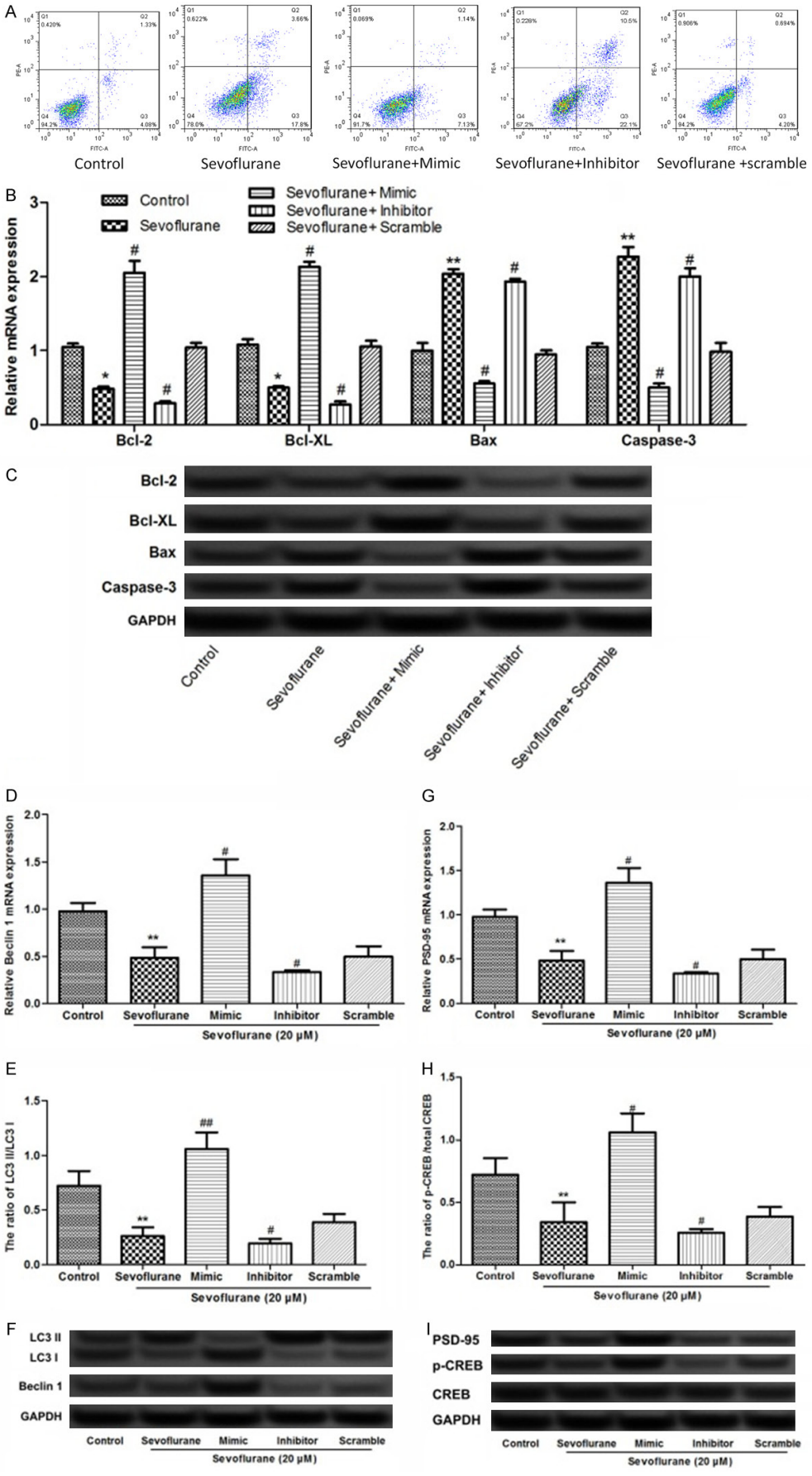
A
Control
Sevoflurane
Sevoflurane+Mimic
Sevoflurane+Inhibitor
Sevoflurane +scramble
B
Control
Sevoflurane
Sevoflurane+ Mimic
Sevoflurane+ Inhibitor
Sevoflurane+ Scramble
Relative mRNA expression
Bcl-2
Bcl-XL
Bax
Caspase-3
C
Bcl-2
Bcl-XL
Bax
Caspase-3
GAPDH
Control
Sevoflurane
Sevoflurane+Mimic
Sevoflurane+Inhibitor
Sevoflurane+Scramble
D
Relative Beclin 1 mRNA expression
Control
Sevoflurane
Mimic
Inhibitor
Scramble
Sevoflurane (20 μM)
G
Relative PSD-95 mRNA expression
Control
Sevoflurane
Mimic
Inhibitor
Scramble
Sevoflurane (20 μM)
E
The ratio of LC3 II/LC3 I
Control
Sevoflurane
Mimic
Inhibitor
Scramble
Sevoflurane (20 μM)
H
The ratio of p-CREB /total CREB
Control
Sevoflurane
Mimic
Inhibitor
Scramble
Sevoflurane (20 μM)
F
LC3 II
LC3 I
Beclin 1
GAPDH
Control
Sevoflurane
Mimic
Inhibitor
Scramble
Sevoflurane (20 μM)
I
PSD-95
p-CREB
CREB
GAPDH
Control
Sevoflurane
Mimic
Inhibitor
Scramble
Sevoflurane (20 μM)

Figure 2. MiR-665 mimic exhibits the neuroprotective effect. A. Cell apoptosis detected using annexin V-Cy5-labeled Apoptosis Detection Kit and analyzed by flow cytometry. Annexin V+/PI-, normal cells; Annexin V+/PI-, early apoptotic cells; Annexin V+/PI+, late apoptotic cells; Annexin V-/PI+, necrotic cells; B, C. The expression of the cell apoptosis related protein in SH-SY5Y cellstransfected with different kinds of miR-665 vectors; D-F. mRNA and protein expression of the cell autophagy related proteins in SH-SY5Y cells; G-I. mRNA and protein expression of the neuron growth related protein in SH-SY5Y cells. * and **indicate difference at $P < 0.05$ and $P < 0.01$, vs. control, respectively. # and ##indicate difference at $P < 0.05$ and $P < 0.01$, vs. sevoflurane, respectively.

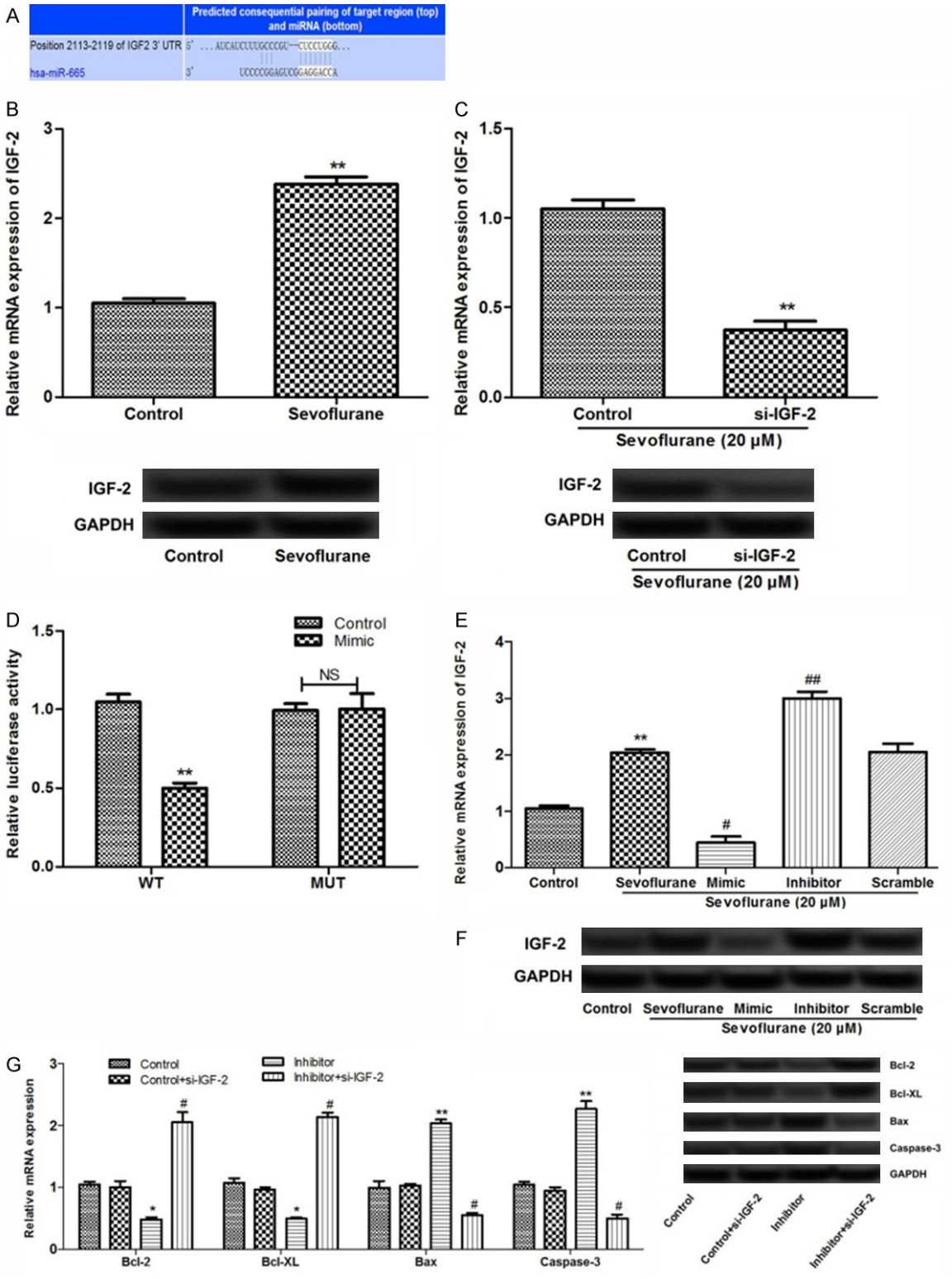

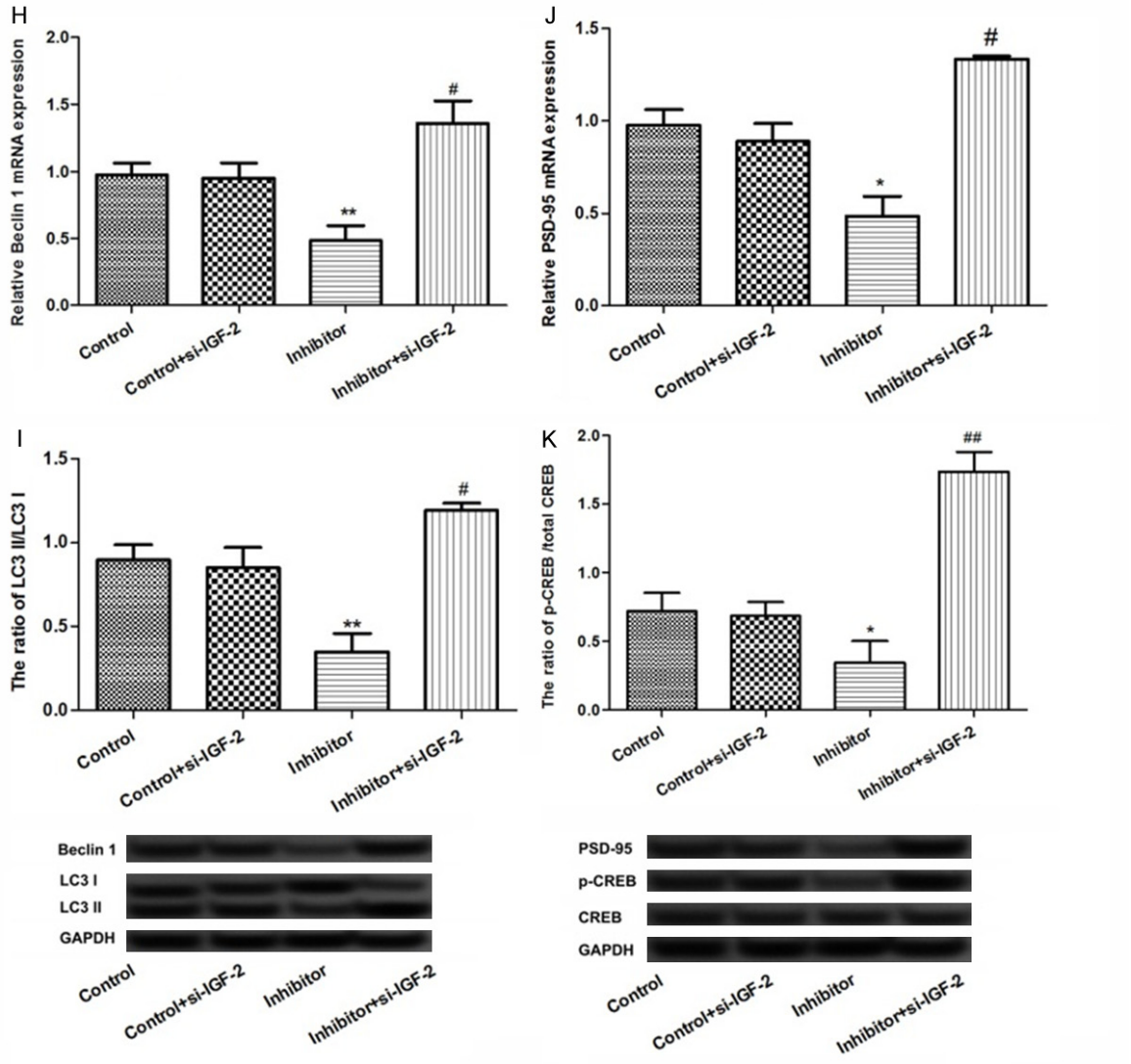

Figure 3. Neuroprotective effect of miR-665 by targeting IGF-2. (A) IGF-2 predicted as the target of miR-665 using TargetScan Human (A: http://www.targetscan.org/vert_71/); (B) Expression of IGF-2 in the SH-SY5Y cells treated with or without sevoflurane; (C) IGF-2 expression in sevoflurane-treated SH-SY5Y cells transfected with or without the silenced IGF-2 vector; (D) Dual-luciferase reporter analysis; (E, F) Expression of IGF-2 in the cells transfected with different kinds of miR-665 vectors; (G, K) The expression, in the SH-SY5Y cells, of the genes related to apoptosis (G), autophagy (H, I), and synaptic growth (J, K) by qRT-PCR and Western blotting. * and **indicate difference at $P < 0.05$ and $P < 0.01$, vs. control, respectively. # and ##indicate difference at $P < 0.05$ and $P < 0.01$, vs. sevoflurane or inhibitor, respectively.

0.05). Subsequently, a concentration of 20 μM to treat SH-SY5Y cells for the *in vitro* experiment was selected. Next, SH-SY5Y cells pretreated with sevoflurane were transfected with miR-665 mimic, inhibitor, and scramble to delineate the miR-665 dysregulation related mechanism (**Figure 1B**).

MiR-665 mimic exhibits neuroprotective effect

An apoptosis assay was employed to confirm the overexpression of miR-665 inhibited sevoflurane-induced apoptosis of SH-SY5Y cells (**Figure 2A-C**), attenuated sevoflurane-inhibited cell autophagy (**Figure 2D-F**), and promoted SH-SY5Y cell growth (**Figure 2G-I**). SH-SY5Y cells transfected with miR-665 mimic significantly reduced Annexin V+/PI- cell percentage (early apoptotic cells), upregulated Bcl-2 and Bcl-xL expression, and down inhibited Bax and Caspase-3 expression in sevoflurane-treated SH-SY5Y cells. Furthermore, the miR-665 mimic clearly triggered the expression of autophagy factors including Beclin-1 and LC3 II/

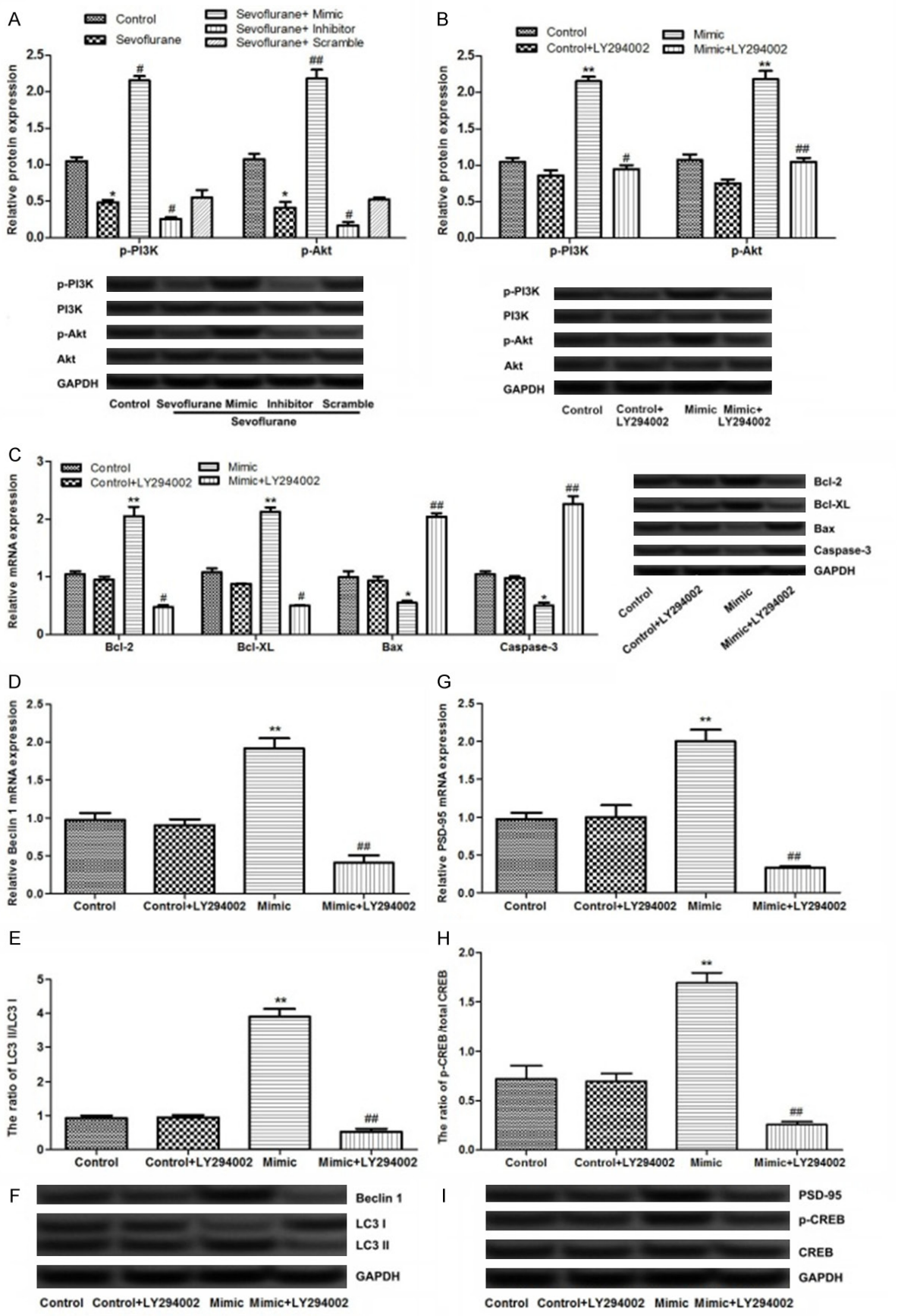
A
Control
Sevoflurane
Sevoflurane+ Mimic
Sevoflurane+ Inhibitor
Sevoflurane+ Scramble
Relative protein expression
p-PI3K
p-Akt
p-PI3K
PI3K
p-Akt
Akt
GAPDH
Control Sevoflurane Mimic Inhibitor Scramble
Sevoflurane
B
Control
Control+LY294002
Mimic
Mimic+LY294002
Relative protein expression
p-PI3K
p-Akt
p-PI3K
PI3K
p-Akt
Akt
GAPDH
Control Control+ LY294002 Mimic Mimic+ LY294002
C
Control
Control+LY294002
Mimic
Mimic+LY294002
Relative mRNA expression
Bcl-2
Bcl-XL
Bax
Caspase-3
Bcl-2
Bcl-XL
Bax
Caspase-3
GAPDH
Control
Control+LY294002
Mimic
Mimic+LY294002
D
Relative Beclin 1 mRNA expression
Control
Control+LY294002
Mimic
Mimic+LY294002
G
Relative PSD-95 mRNA expression
Control
Control+LY294002
Mimic
Mimic+LY294002
E
The ratio of LC3 II/LC3 I
Control
Control+LY294002
Mimic
Mimic+LY294002
H
The ratio of p-CREB /total CREB
Control
Control+LY294002
Mimic
Mimic+LY294002
F
Beclin 1
LC3 I
LC3 II
GAPDH
Control Control+LY294002 Mimic Mimic+LY294002
I
PSD-95
p-CREB
CREB
GAPDH
Control Control+LY294002 Mimic Mimic+LY294002

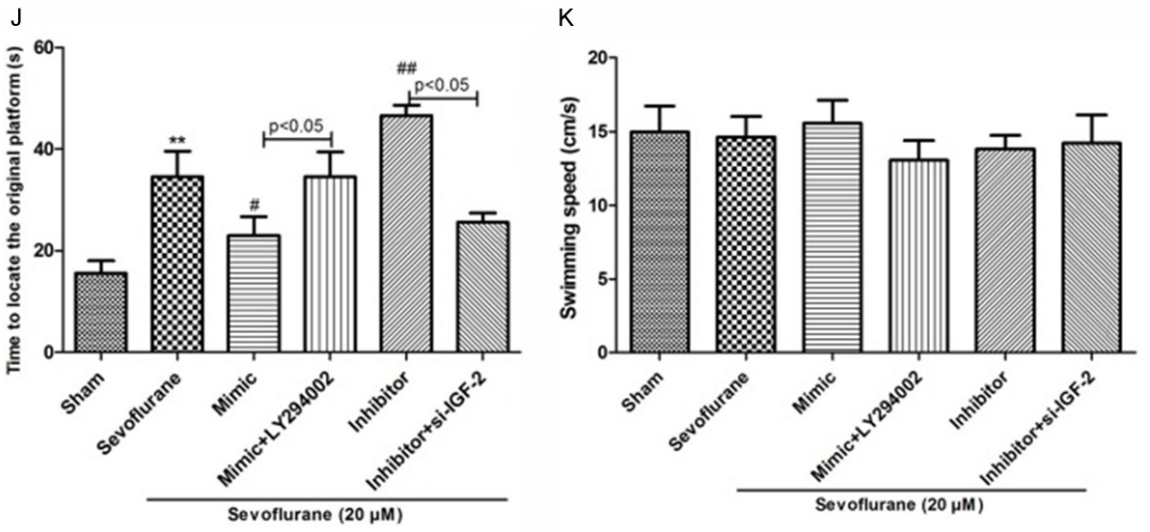

Figure 4. MiR-665-mediated neuroprotective effect associates with PI3K/Akt signal pathway. (A) PI3K/Akt signaling pathway related protein expression in the sevoflurane-treated SH-SY5Y cells; (B) Expression of the PI3K/Akt signaling pathway related protein in the sevoflurane-treated SH-SY5Y cells with P13K/Akt inhibitor LY294002; (C, I) expression of neuron apoptosis (C), autophagy (D-F), and synaptic growth (G-I) related proteins in the sevoflurane-treated SH-SY5Y cells. * and **indicate $P < 0.05$ and $P < 0.01$, vs. control, respectively. # and ##indicate $P < 0.05$ and $P < 0.01$, vs. sevoflurane or mimic, respectively; (J, K) MiR-665 mimic and siRNA-IGF-2 improving animal latency time. Male SD rats were treated with sevoflurane, miR-665 mimic, inhibitor, siRNA-IGF-2, and LY294002. Rat motor performance was tested using the Morris water maze task. The time taken by the rats to find the hidden platform (latency, s, A), and swimming speeds ($cm \cdot s^{-1}$, B) were detected. **$P < 0.01$, vs. Control (namely, the Sham group). # and ##$P < 0.05$ and $P < 0.01$, vs. cells treated with sevoflurane or mimic, respectively.

LC3 I ratio in sevoflurane-treated SH-SY5Y cells. Finally, we analyzed the effect of miR-665 mimic on the development of neurons and revealed that miR-665 expression remarkably upregulated the expression of PSD-95 and pCREB. An administration of the inhibitor intensified the influence of sevoflurane on cell functions and the expression of the above factors. No differences were found in the expression and cellular performance among the cells treated with the scramble. This demonstrated that miR-665 benefits in preventing sevoflurane-induced neuron apoptosis, autophagy recession, and synaptic growth inhibition.

Neuroprotective effect of miR-665 by targeting IGF-2

We predicted IGF-2 as one of the miR-665 targets using TargetScan Human (**Figure 3A**), and subsequently, using the Firefly/Renilla dual-luciferase reporter systems, determined that IGF-2 is a negative target of miR-665. In contrast to the downregulated miR-665 expression, IGF-2 was triggered by sevoflurane treatment and miR-665 inhibitor, and inhibited by miR-665 mimic (**Figure 3B** and **3C**). Using the dual-luciferase reporter assay, it was revealed that miR-665 administration reduced firefly-luciferase activity ratio in the cells transfected with pGL3-IGF-2-WT-3'-UTR vector (**Figure 3D**). Further, the cotransfection experiments with IGF-2 siRNA and miR-665 inhibitor into SH-SY5Y cells showed an upregulation of the Bcl-2, Bcl-xL, Beclin-1, LC3 II, PSD-95, and p-CREB expressions, and a downregulation of the Bax, Caspase-3 and LC3 I expressions, compared to the transfection of miR-665 inhibitor alone (**Figure 3E-I**). These data indicated that miR-665 regulates the neuron apoptosis, autophagy, and synaptic growth by negatively targeting IGF-2.

MiR-665-mediatedneuron proliferation associates with PI3K/Akt signal pathway

Prior studies have shown that sevoflurane is linked to P13k/Akt signaling pathway [6, 33]. In order to test whether the neuroprotective effect of miR-665 against sevoflurane is due to the activation of PI3K/Akt pathway, we inhibited the P13K/Akt signaling pathway using LY294002-aninhibitor against P13K/Akt signaling pathway [34]. The P13K/Akt signaling

pathway was inactivated by sevoflurane but activated by miR-665 mimic transfection (**Figure 4A**). However, the expression of p-PI3K and p-Akt triggered by miR-665 mimic could be inhibited by LY294002. Next, we found that P13K/Akt inhibitor LY294002 reversed the miR-665 mimic induced changes in neuron apoptosis, autophagy recession, and the synaptic growth related proteins (**Figure 4C-I**). LY294002 inhibited the miR-665 triggered increase in Bcl-2, Bcl-xL, Beclin 1, and PSD-95 expressions and the upregulation of LC3 II/LC3 I and p-CREB/CREB ratios. Furthermore, LY294002 attenuated miR-665-induced decrease in Bax and Caspase-3 expressions (**Figure 4C**). However, there were no differences in the expression of these factors between control cells and those treated with LY294002 (**Figure 4B-I**). These data confirm that sevoflurane-inhibited neuron proliferation and the development via miR-665 were dependent on PI3K/Akt signaling pathway.

MiR-665 mimic and siRNA-IGF-2 improve animal performance

In order to delineate the neuroprotective effect of miR-665 against sevoflurane under *in vivo* conditions, the anesthetized rats with sevoflurane were tested for their performance using MWM task (**Figure 4**). The time taken to find the hidden platform (latency, s) was significantly different among the groups (**Figure 4J**). The rats treated with sevoflurane alone or with-miR-665 inhibitor showed a high latency time ($P < 0.01$). On the contrary, miR-665 mimic and siRNA-IGF-2 transfected rats showed a low latency time ($P < 0.05$). The administration of P13K/Akt signaling pathway inhibitor LY294002 reversed the influence of miR-665 mimic on rats by increasing latency time. No differences were found in swimming speed among the rats (**Figure 4K**). These data showed that miR-665 expression canceled out the sevoflurane-induced behavior deficits via IGF-2 and P13K/Akt signaling pathway.

Discussion

Anesthesia-induced cognitive impairment is probably the most frequent type of postoperative cognitive impairment, which has been found to be associated with miRNA dysregulation [35]. This study was aimed to investigate the effect of miR-665 expression on sevoflurane anesthesia-induced cognitive impairment. We confirmed the neuroprotective effect of miR-665 against sevoflurane anesthesia by targeting IGF-2 and activating P13K/Akt signaling pathways. A miR-665 mimic reversed the sevoflurane-induced neuroapoptosis, autophagy inhibition, and the motor deficits in rats by negatively targeting IGF-2 via P13K/Akt signaling pathway.

In an earlier study, propofol anesthesia triggered the expression of miR-665 in the hippocampal neuron of rats, which was accompanied with the downregulation of Bcl-xL [14]. However, in our study, the sevoflurane-anesthetized rats showed decreased miR-665 expression with a decrease in Bcl-xL and Bcl-2 expressions and increase in IGF-2 expression. Taken together, it can be concluded that propofol induces upregulation of miR-665 [14], while sevoflurane anesthesia decreases miR-665 expression as observed in our study. However, both anesthetics promoteneurons apoptosis and postoperative cognitive impairment in rats. This might due to the fact that sevoflurane and propofol differentially changed the expression levels of miRNAs in rat hippocampus [36, 37].

Using the TargetScan Human [38], we predicted and confirmed that IGF-2 serves as the direct target of miR-665 (**Figure 2**). IGF-2 activates the PI3K/AKT pathway, and IGF-2/P13K/Akt signaling cascade is involved in autophagy and apoptosis [39]. As earlier reported, IGF-2 stimulates IGF1R and subsequently PI3K/Akt and MAPK/ERK signaling, and increases IGF-2 levels accompanied with the activation of ERK1/2 [40, 41]. Moreover, LY294002, a P13K/Akt signaling inhibitor, could prevent IGF-2-mediated gene modulations [42, 43], demonstrating that IGF-2 mediated PI3K/Akt signaling is essential for cell functions. In this study, we confirmed that IGF-2 is a direct target of miR-665, suggesting the crucial roles of miR-665 in PI3K/Akt pathway related activities via targeting IGF-2.

PI3K/Akt signaling pathway dysregulation is involved in the cognitive impairment induced by diabetes, neonatal hypoxic-ischemic brain damage, cardiovascular disease, and anesthesia [44]. The activation of PI3K/Akt signaling pathway is crucial for neuroapoptosis and autophagy, and its inhibition accelerates hippocampal

neuroapoptosis and reduces regular autophagy through targeting apoptosis-related proteins or interaction with other signaling pathways [45, 46]. For instance, Yoshii et al. revealed that the inhibition of MAPK/ERK signaling pathway disrupted PSD95 expression, which is required for p-P13K and p-CREB participations [47]. Moreover, the p-CREB-dependent Bcl-2 signaling, essential for cell apoptosis, is required for PSD95 disruption [47]. In the present study, we determined that sevoflurane anesthesia inhibited miR-655 was accompanied with a concomitant decrease in PI3K/Akt activation, Bcl-2 and Bcl-xL expressions, and regular autophagy along with an increase in Bax and Caspase-3 expressions. All of these changes, however, could be reversed by miR-665 mimic transfection. These indicated that miR-665-mediated neuroprotective effect is linked with the upregulation of the Bcl-2 cascade through P13K/Akt signaling pathway by targeting IGF-2.

Disclosure of conflict of interest

None.

Address correspondence to: Xihua Lu, Department of Anesthesiology, Affiliated Cancer Hospital of Zhengzhou University, Henan Cancer Hospital Anesthesiology, No.127 Dongming Road, Zhengzhou 450003, Henan, China. E-mail: xihualu209@yeah.net

References

[1] Parrott MD, Winocur G, Bazinet RP, Ma DW and Greenwood CE. Whole-food diet worsened cognitive dysfunction in an Alzheimer's disease mouse model. Neurobiol Aging 2015; 36: 90-99.

[2] Ng C. Adiponectin deficiency induced cognitive dysfunction and Alzheimer's disease pathogenesis in mice through the disruption of insulin sensitivity and inactivated AMPK signaling. In Annual Meeting of the American Academy of Neurology, AAN 2015; 2015.

[3] Rundshagen I. Postoperative cognitive dysfunction. Dtsch Arztebl Int 2014; 111: 119-125.

[4] Grape S, Ravussin P, Rossi A, Kern C and Steiner L. Postoperative cognitive dysfunction. Trends in Anaesthesia and Critical Care 2012; 2: 98-103.

[5] Vogelstein B and Kinzler KW. Cancer genes and the pathways they control. Nat Med 2004; 10: 789-799.

[6] Ye Z, Xia P, Cheng ZG and Guo Q. Neuroprotection induced by sevoflurane-delayed postconditioning is attributable to increased phosphorylation of mitochondrial GSK-3β through the PI3K/Akt survival pathway. J Neurol Sci 2015; 348: 216-225.

[7] Wang WY, Yang R, Hu SF, Wang H, Ma ZW and Lu Y. N-stearoyl-l-tyrosine ameliorates sevoflurane induced neuroapoptosis via MEK/ERK1/2 MAPK signaling pathway in the developing brain. Neurosci Lett 2013; 541: 167-172.

[8] Wang WY, Jia LJ, Yan L, Zhang HH, Fang C, Hui M, Xu WC, Fang JB, Peng ZY and Ma ZW. Location- and subunit-specific NMDA receptors determine the developmental sevoflurane neurotoxicity through ERK1/2 signaling. Mol Neurobiol 2014; 53: 216-230.

[9] Dong J, Wang Y, Wang Y, Wei W, Min H, Song B, Xi Q, Teng W and Chen J. Iodine deficiency increases apoptosis and decreases synaptotagmin-1 and PSD-95 in rat hippocampus. Nutr Neurosci 2013; 16: 135-141.

[10] Zuo H, Lin T, Wang D, Peng R, Wang S, Gao Y, Xu X, Zhao L, Wang S and Su Z. RKIP regulates neural cell apoptosis induced by exposure to microwave radiation partly through the MEK/ERK/CREB pathway. Mol Neurobiol 2015; 51: 1520-1529.

[11] Takeda K, Kermani P, Anastasia A, Obinata Y, Hempstead BL and Kurihara H. BDNF protects human vascular endothelial cells from TNFα-induced apoptosis. Biochem Cell Biol 2013; 91: 341-349.

[12] Welch C, Chen Y and Stallings R. MicroRNA-34a functions as a potential tumor suppressor by inducing apoptosis in neuroblastoma cells. Oncogene 2007; 26: 5017-5022.

[13] Zhao L, Gu H, Chang J, Wu J, Wang D, Chen S, Yang X and Qian B. MicroRNA-383 regulates the apoptosis of tumor cells through targeting Gadd45g. PLoS One 2014; 9: e110472.

[14] Sun WC and Pei L. rno-miR-665 targets BCL-2L1 (Bcl-xl) and increases vulnerability to propofol in developing astrocytes. J Neurochem 2016; 138: 233-242.

[15] Barry G. Integrating the roles of long and small non-coding RNA in brain function and disease. Mol Psychiatry 2014; 19: 410-416.

[16] Backes C, Meese E and Keller A. Specific miRNA disease biomarkers in blood, serum and plasma: challenges and prospects. Mol Diag Ther 2016; 20: 509-518.

[17] Shang Y, Zang A, Li J, Jia Y, Li X, Zhang L, Huo R, Yang J, Feng J and Ge K. MicroRNA-383 is a tumor suppressor and potential prognostic biomarker in human non-small cell lung caner. Biomed Pharmacother 2016; 83: 1175-1181.

[18] Gao W, Lu X, Liu L, Xu J, Feng D and Shu Y. MiRNA-21: a biomarker predictive for platinum-based adjuvant chemotherapy response in patients with non-small cell lung cancer. Cancer Biol Ther 2012; 13: 330-340.
[19] Lai NS, Wu DG, Fang XG, Lin YC, Chen SS, Li ZB and Xu SS. Serum microRNA-210 as a potential noninvasive biomarker for the diagnosis and prognosis of glioma. Br J Cancer 2015; 112: 1241-1246.
[20] Endo K, Naito Y, Ji X, Nakanishi M, Noguchi T, Goto Y, Nonogi H, Ma X, Weng H and Hirokawa G. MicroRNA 210 as a biomarker for congestive heart failure. Biol Pharm Bull 2013; 36: 48-54.
[21] Li X, Wu G, Wang S, Huang P, Cao X and He J. Circulating miR-665 and miR-30c-1-3p, the candidate markers of congestive heart failure with qi-deficiency-blood-stasis syndrome. International Journal of Clinical and Experimental Medicine 2016; 9: 11675-11679.
[22] Sun WC, Liang ZD and Pei L. Propofol-induced rno-miR-665 targets BCL2L1 and influences apoptosis in rodent developing hippocampal astrocytes. Neurotoxicology 2015; 51: 87-95.
[23] Yu X, Liu S, Li J, Fan X, Chen Y, Bi X and Deng X. MicroRNA-572 improves early post-operative cognitive dysfunction by down-regulating neural cell adhesion molecule 1. PLoS One 2015; 10: 1681-1682.
[24] Chen J, Jiao Z, Wang A, Zhong W, Liu B and Gan N. MicroRNA-181 inhibitor protects against sevoflurane-induced hippocampal apoptosis and memory impairment. International Journal of Clinical and Experimental Pathology 2016; 9: 6195-6202.
[25] Tu Y, Wan L, Fan Y, Wang K, Bu L, Huang T, Cheng Z and Shen B. Ischemic postconditioning-mediated miRNA-21 protects against cardiac ischemia/reperfusion injury via PTEN/Akt pathway. PLoS One 2013; 8: e75872-e75872.
[26] He Z, Cen D, Luo X, Li D, Li P, Liang L and Meng Z. Downregulation of miR-383 promotes glioma cell invasion by targeting insulin-like growth factor 1 receptor. Med Oncol 2013; 30: 1-6.
[27] Lee J, Ahn E, Park WK and Park S. Phosphoproteome profiling of SH-SY5y neuroblastoma cells treated with anesthetics: sevoflurane and isoflurane affect the phosphorylation of proteins involved in cytoskeletal regulation. PLoS One 2016; 11: e0162214.
[28] Zhang H, Gao Y, Zhao FL, Qiao PF and Yan Y. Hydrogen sulfide-induced processing of the amyloid precursor protein in SH-SY5Y human neuroblastoma cells involves the PI3-K/Akt signaling pathway. Cell Mol Neurobiol 2015; 35: 265-272.
[29] Liu DZ, Jickling GC, Ander BP, Hull H, Zhan X, Cox C, Shroff N, Dykstraaiello C, Stamova B and Sharp FR. Elevating microRNA-122 in blood improves outcomes after temporary middle cerebral artery occlusion in rats. J Cereb Blood Flow Metab 2016; 36: 1374-1383.
[30] Jie L, Su M, Ke W, Cao J, Wang B, Ping L, Dong J and Liu Y. Propofol prevents electroconvulsive-shock-induced memory impairment through regulation of hippocampal synaptic plasticity in a rat model of depression. Neuropsychiatr Dis Treat 2014; 10: 1847-1859.
[31] Shynkar VV, Klymchenko AS, Kunzelmann C, Duportail G, Muller CD, Demchenko AP, Freyssinet JM and Mely Y. Fluorescent biomembrane probe for ratiometric detection of apoptosis. J Am Chem Soc 2007; 129: 2187-2193.
[32] Laurent-Rolle M, Morrison J, Rajsbaum R, Macleod JL, Pisanelli G, Pham A, Ayllon J, Miorin L, Martínez-Romero C and Tenoever B. The interferon signaling antagonist function of yellow fever virus NS5 protein is activated by type I interferon. Cell Host Microbe 2014; 16: 314-327.
[33] Ye Z, Guo Q, Xia P, Wang N, Wang E and Yuan Y. Sevoflurane postconditioning involves an up-regulation of HIF-1α and HO-1 expression via PI3K/Akt pathway in a rat model of focal cerebral ischemia. Brain Res 2012; 1463: 63-74.
[34] Chen L, Han L, Shi Z, Zhang K, Liu Y, Zheng Y, Jiang T, Pu P, Jiang C and Kang C. LY294002 enhances cytotoxicity of temozolomide in glioma by down-regulation of the PI3K/Akt pathway. Mol Med Rep 2012; 5: 575-579.
[35] Luo T, Yin S, Shi R, Xu C, Wang Y, Cai J, Yue Y and Wu A. miRNA expression profile and involvement of Let-7d-APP in aged rats with isoflurane-induced learning and memory impairment. PLoS One 2015; 10: e0119336.
[36] Ishikawa M, Tanaka S, Arai M, Genda Y and Sakamoto A. Differences in microRNA changes of healthy rat liver between sevoflurane and propofol anesthesia. Anesthesiology 2012; 117: 1245-1252.
[37] Goto G, Hori Y, Ishikawa M, Tanaka S and Sakamoto A. Changes in the gene expression levels of microRNAs in the rat hippocampus by sevoflurane and propofol anesthesia. Mol Med Rep 2014; 9: 1715-1722.
[38] Wei Y, Cui YF, Tong HL, Zhang WW and Yan YQ. MicroRNA-2400 promotes bovine preadipocyte proliferation. Biochem Biophys Res Commun 2016; 478: 1054-1059.
[39] Shimizu T, Sugihara E, Yamaguchi-Iwai S, Tamaki S, Koyama Y, Kamel W, Ueki A, Ishikawa T, Chiyoda T and Osuka S. IGF2 preserves osteosarcoma cell survival by creating an autophagic state of dormancy that protects cells against chemotherapeutic stress. Cancer Res 2014; 74: 6531-6541.

[40] Yeh CC, Sun HL, Huang CJ, Wong CS, Cherng CH, Huh BK, Wang JS and Chien CC. Long-term anti-allodynic effect of immediate pulsed radiofrequency modulation through down-regulation of insulin-like growth factor 2 in a neuropathic pain model. Int J Mol Sci 2015; 16: 27156-27170.
[41] Lewis BC. Abstract IA6: identification and characterization of factors required for KRAS-driven pancreatic tumorigenesis. Cancer Research 2015; 75: IA6-IA6.
[42] Thomas D. The role of IGF2 in the regulation of hematopoietic stem cell function. 2014.
[43] Tominaga K, Shimamura T, Kimura N, Murayama T, Matsubara D, Kanauchi H, Niida A, Shimizu S, Nishioka K and Tsuji E. Addiction to the IGF2-ID1-IGF2 circuit for maintenance of the breast cancer stem-like cells. Oncogene 2017; 36: 1276-1286.
[44] Wang Y, Wu C, Han B, Xu F, Mao M, Guo X and Wang J. Dexmedetomidine attenuates repeated propofol exposure-induced hippocampal apoptosis, PI3K/Akt/Gsk-3β signaling disruption, and juvenile cognitive deficits in neonatal rats. Mol Med Rep 2016; 14: 769-775.
[45] Brunet A, Datta SR and Greenberg ME. Transcription-dependent and-independent control of neuronal survival by the PI3K-Akt signaling pathway. Curr Opin Neurobiol 2001; 11: 297-305.
[46] Luo L, Liu XL, Li J, Mu RH, Liu Q, Yi LT and Geng D. Macranthol promotes hippocampal neuronal proliferation in mice via BDNF-TrkB-PI3K/Akt signaling pathway. Eur J Pharmacol 2015; 762: 357-363.
[47] Yoshii A and Constantine-Paton M. Postsynaptic localization of PSD-95 is regulated by all three pathways downstream of TrkB signaling. Front Synaptic Neurosci 2014; 6: 6.